

A Broad-Band, Automated, stripline Technique for the Simultaneous Measurement of Complex Permittivity and Permeability

WALTER BARRY

Abstract—A broad-band automated technique for making frequency-swept measurements of complex permittivity and permeability simultaneously is described. ϵ_r and μ_r are computed from S -parameter measurements made on a strip transmission-line device loaded with the material under test. The derivation of ϵ_r and μ_r as functions of S_{11} and S_{21} is included, as well as a practical design for a stripline sample holder. Measured ϵ_r and μ_r data for several dielectrics and ceramic ferrites is also presented. The technique has been found to have an overall accuracy of better than ± 5 percent.

I. INTRODUCTION

THIS PAPER PRESENTS a method for simultaneously measuring the real and imaginary components of both permittivity (ϵ) and permeability (μ) of a given material. The general method, previously referred to by Weir [1], makes use of the complex S -parameters measured for a waveguide or transmission line loaded with the material under test to calculate ϵ and μ . The technique described here employs a strip transmission-line fixture into which blocks of the material to be measured may be inserted easily. An automated network analyzer system is used to make frequency-swept S -parameter measurements on the loaded stripline fixture from which complex ϵ and μ may be calculated. The measurement technique was developed to characterize accurately the electromagnetic properties of certain ceramic ferrites in the 0.5–5.5-GHz frequency band. These ferrites are to be used for RF signal attenuation between pickups and kickers in the beam cooling rings of the antiproton source at the Fermi National Laboratory [2]. The ability to measure electric and magnetic parameters simultaneously makes the automated stripline technique ideal for this application, as well as for measuring the properties of materials for general electromagnetic applications.

Manuscript received February 21, 1985; revised July 22, 1985. This work was supported in part by the Office of Energy Research, Office of High Energy and Nuclear Physics, High Energy Physics Division, U.S. Department of Energy, under Contract DE-AC03-76SF00098.

The author is with the Lawrence Berkeley Laboratory, University of California, Berkeley, CA 94720.

IEEE Log Number 8405811.

II. THEORY

The diagram in Fig. 1 represents a strip transmission line of length $2l + t$ loaded in the center with a material of length t and unknown complex relative permittivity and permeability

$$\epsilon_r = \epsilon'_r - j\epsilon''_r$$

$$\mu_r = \mu'_r - j\mu''_r.$$

The stripline has a characteristic impedance of Z_0 (free-space regions I and III) which when loaded with the sample material (region II) becomes Z , where

$$Z = Z_0 \sqrt{\frac{\mu_r}{\epsilon_r}}. \quad (1)$$

In the unloaded regions, the propagation constant is $k_0 = \omega\sqrt{\mu_0\epsilon_0}$, while in the loaded region, the propagation constant is generally complex and is designated by k , where

$$k = k_0 \sqrt{\mu_r \epsilon_r}. \quad (2)$$

At the plane boundaries between regions I and II, and regions II and III, there are complex reflection coefficients R and $-R$, respectively, where

$$R = \frac{Z - Z_0}{Z + Z_0}. \quad (3)$$

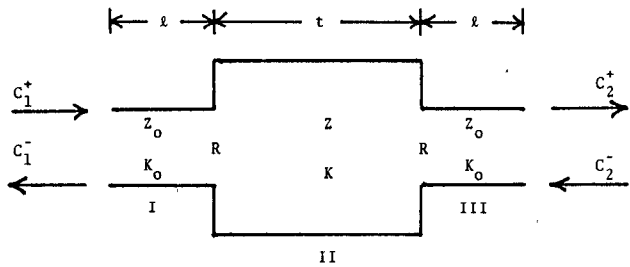
Using (1), equations (2) and (3) may be solved simultaneously to yield the desired parameters

$$\epsilon_r = \frac{k}{k_0} \left(\frac{1 - R}{1 + R} \right) \quad (4)$$

$$\mu_r = \frac{k}{k_0} \left(\frac{1 + R}{1 - R} \right). \quad (5)$$

Thus, knowing k and R enables ϵ_r and μ_r to be calculated. The values for k and R may be found from the values of S_{11} and S_{21} measured at the input (far left of region I) and output (far right of region III) terminals in Fig. 1.

In order to relate k and R to the measured S -parameters, consider the relationship between the forward and reverse voltages [3] at the input terminals C_1^+ and C_1^- , and

Fig. 1. Diagram for determining *S*-parameters.

at the output terminals C_2^+ and C_2^-

$$\begin{bmatrix} C_1^+ \\ C_1^- \end{bmatrix} = \begin{bmatrix} T_{11} & T_{12} \\ T_{21} & T_{22} \end{bmatrix} \begin{bmatrix} C_2^+ \\ C_2^- \end{bmatrix} \quad (6)$$

where the matrix $[T]$ is the total wave amplitude matrix for the "device" in Fig. 1. The elements of $[T]$ may be found by multiplying the wave amplitude matrix for each transmission section and reflection as follows:

$$\begin{aligned} [T] = & \begin{bmatrix} e^{jk_0 l} & 0 \\ 0 & e^{-jk_0 l} \end{bmatrix} \begin{bmatrix} (1-R)^{-1} & R(1-R)^{-1} \\ R(1-R)^{-1} & (1-R)^{-1} \end{bmatrix} \cdot \\ & \cdot \begin{bmatrix} e^{jkt} & 0 \\ 0 & e^{-jkt} \end{bmatrix} \begin{bmatrix} (1+R)^{-1} & -R(1+R)^{-1} \\ -R(1+R)^{-1} & (1+R)^{-1} \end{bmatrix} \cdot \\ & \cdot \begin{bmatrix} e^{jk_0 l} & 0 \\ 0 & e^{-jk_0 l} \end{bmatrix}. \end{aligned} \quad (7)$$

After multiplying, the elements of $[T]$ are found to be

$$\begin{bmatrix} T_{11} & T_{12} \\ T_{21} & T_{22} \end{bmatrix} = \frac{1}{(1-R^2)} \cdot \begin{bmatrix} e^{j2k_0 l}[e^{jkt} - R^2 e^{-jkt}] & -j2R \sin kt \\ j2R \sin kt & e^{-j2k_0 l}[e^{-jkt} - R^2 e^{jkt}] \end{bmatrix} \quad (8)$$

and are related to the *S*-parameters as follows:

$$\begin{bmatrix} T_{11} & T_{12} \\ T_{21} & T_{22} \end{bmatrix} = \begin{bmatrix} 1/S_{12} & -S_{22}/S_{12} \\ S_{11}/S_{12} & (S_{12}^2 - S_{11}S_{22})/S_{12} \end{bmatrix}. \quad (9)$$

Thus, the *S*-parameters are found to be

$$S_{21} = S_{12} = \frac{(1-R^2)e^{-j2k_0 l}}{e^{jkt} - R^2 e^{-jkt}} \quad (10)$$

$$S_{11} = S_{22} = \frac{j2R e^{-j2k_0 l} \sin kt}{e^{jkt} - R^2 e^{-jkt}}. \quad (11)$$

Equations (10) and (11) may now be solved simultaneously for kt and R in terms of the known and measured quantities

$$kt = \cos^{-1} \left(\frac{e^{-j4k_0 l} + S_{12}^2 - S_{11}^2}{2e^{-j2k_0 l}S_{12}} \right) = \cos^{-1}(\arg) \quad (12)$$

$$R = S_{11} / (e^{-j2k_0 l} - S_{12} e^{-jkt}) \quad (13)$$

and ϵ_r and μ_r may be obtained through (4) and (5).

Because of the large number of complex arithmetic operations involved, a certain amount of care must be

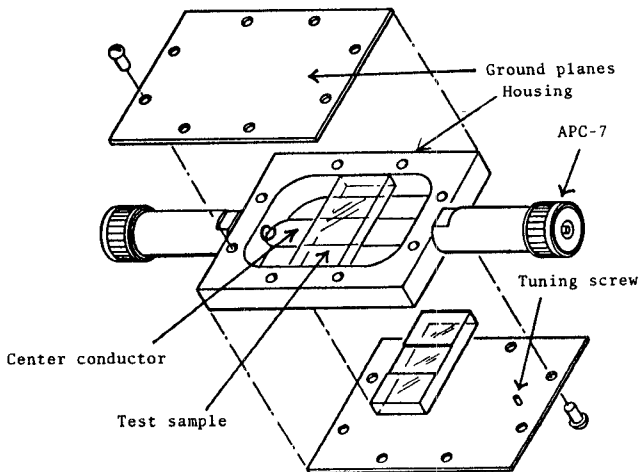


Fig. 2. Stripline measurement device.

taken when using (12) in practice. When resolved into its real and imaginary components, (12) becomes

$$kt_{\text{real}} = \Theta_G \pm 2n\pi, \quad n = 0, 1, 2, \dots \quad (14)$$

$$kt_{\text{imag}} = \ln G \quad (15)$$

where Θ_G and G are real numbers defined as follows:

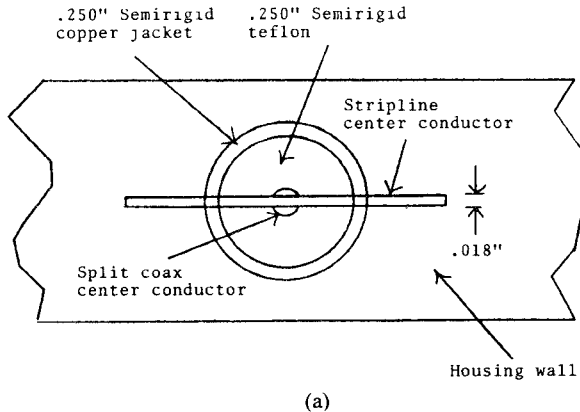
$$\Theta_G = \tan^{-1} \left[\text{Im} \left(\arg + \sqrt{\arg^2 - 1} \right) \right] / \text{Re} \left(\arg + \sqrt{\arg^2 - 1} \right) \quad (16)$$

$$G = \left(\left[\text{Re} \left(\arg + \sqrt{\arg^2 - 1} \right) \right]^2 + \left[\text{Im} \left(\arg + \sqrt{\arg^2 - 1} \right) \right]^2 \right)^{1/2}. \quad (17)$$

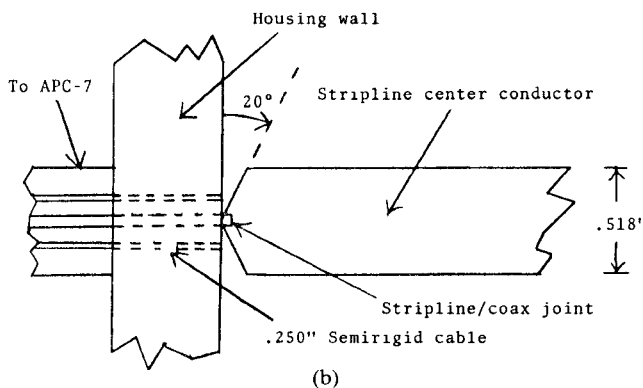
The integral multiple of 2π appearing in (14) is a result of the multivalued inverse cosine function. For material lengths in the range $0 \leq t \leq \lambda_m/2$ (λ_m is wavelength inside the material), the principal branch of \cos^{-1} should be used, i.e., $n = 0$. Since material samples of length $t > \lambda_m/2$ introduce dimensional resonances [4] that invalidate the measured values for S_{11} and S_{21} , all samples were kept to $t < \lambda_m/2$; therefore, the value of $n = 0$ was always correct.

III. STRIPLINE MEASUREMENT DEVICE

The stripline test "chamber" developed for the ϵ and μ measurements is pictured in Fig. 2. The stripline portion of the device was designed for a characteristic impedance of $Z_0 = 50 \Omega$ in order to match that of the cables and network analyzer system used to make the *S*-parameter measurements. The critical dimensions for the stripline chamber are as follows: ground plane separation = 1.000 cm, center conductor width = 1.316 cm, and center conductor thickness = 0.048 cm. Both the ground planes and center conductor are made of a beryllium copper alloy for rigidity, while the housing is made of aluminum with approximate inside dimensions of 6.0 cm \times 4.3 cm \times 1 cm. The test samples which fit above and below the center conductor inside the housing must have dimensions $t \times 4.3$ cm \times .48 cm in order to fit securely. As previously discussed, t must be less than $\lambda_m/2$ in order to avoid dimensional reso-



(a)

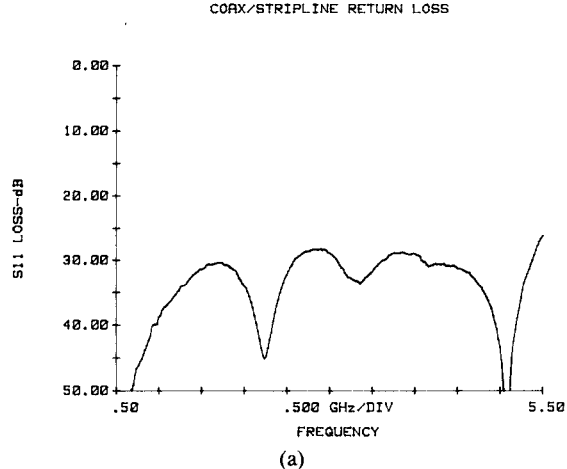


(b)

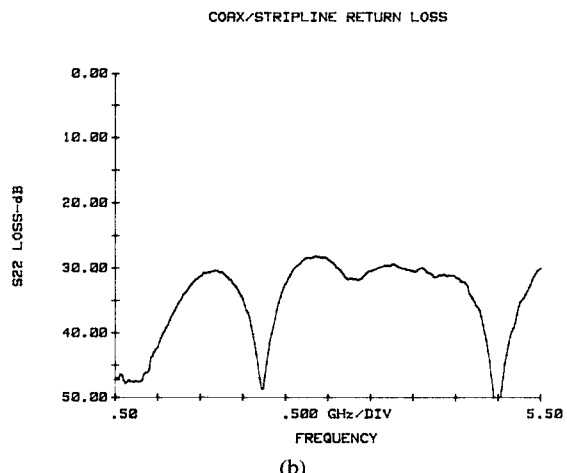
Fig. 3. Coax to stripline connection.

nances. It should be noted that although Fig. 2 indicates grooves in the samples for a better fit around the center conductor, it was found that samples without grooves measured equally well; therefore, the grooves may be deleted in order to save time when preparing samples.

It was a prime concern in developing the test chamber to obtain the best possible transition from the stripline to the network analyzer. This task mainly involved the development of extremely low-reflection connections from stripline to coax. After considerable experimentation, optimum connections were obtained by press fitting standard 0.250-in semirigid cables through the housing walls so that the copper jackets and teflon of the cables were flush with the inside of the walls. The center conductors of the semirigid cables were cut so that they protruded 0.050-in into the chamber and were split with a 0.018-in slitting saw so as to accept the stripline center conductor (see Fig. 3). The stripline center conductor was beveled to a point (20° with respect to the housing wall) to obtain a good match and soldered to the split center conductors of the semirigid cable. Lastly, single-sexed APC-7 connectors were attached to the semirigid cables outside the housing. Capacitive tuning screws which protrude through one of the ground planes over the stripline/coax joints were then adjusted while monitoring reflection with a time-domain reflectometer in order to optimize each match. Return-loss measurements of the resulting device (without test sample) appear



(a)



(b)

Fig. 4. Return loss for each port of empty stripline device.

in Fig. 4. The reflected signal for both ports is better than 30 dB down over most of the 0.5–5.5-GHz band.

IV. PROCEDURE FOR MATERIAL MEASUREMENTS

In order to compute ϵ_r and μ_r correctly, the S -parameters of the empty and loaded test device must be measured to a high degree of accuracy. These measurements were performed with a Hewlett-Packard network analyzer system the main components of which are an 8410C network analyzer, 8746B S -parameter test set, and an 8411A harmonic frequency converter. An HP 9816 computer with appropriate interfacing and peripherals was used for automation, data acquisition, computations, and printing/plotting.

The first step in the measurement procedure is to calibrate out certain errors associated with the S -parameter test set and cables leading to the stripline device to be measured. This is done by performing the standard 12-term error correction calibration procedure for the HP network analyzer. Once the system is calibrated, S_{12} for the stripline device is measured so its total electrical length may be determined from the phase data. The length parameter l may then be computed by subtracting the physical thickness t of the sample to be tested from the total electrical

length and dividing by two. With the test sample centered in the device, all four *S*-parameters are measured. The rms averages of S_{11} and S_{22} , and S_{12} and S_{21} are then used to compute ϵ_r and μ_r , with (12), (13), (4), and (5). Although the device is theoretically symmetric, the average reflection and transmission parameters are used to help compensate for errors in centering the samples. In order to assess the sensitivity of the measurements to sample centering, measurements of the same samples were repeated after recentering several times. The data indicated no difference in either the *S*-parameters themselves or the computed values of ϵ_r and μ_r (apart from random noise errors). A provision for calculating the electrical length of the sample as a function of frequency was also included to ensure it did not exceed $\lambda_m/2$ at any point.

V. ϵ_r AND μ_r MEASUREMENTS

For the purpose of assessing the accuracy of the measurement technique, the first materials to be measured were three dielectrics with well-known properties: polyethylene, teflon, and lucite. The results of these measurements for the 0.5–5.5-GHz band appear in Fig. 5. The real parts of ϵ_r and μ_r , in both Figs. 5 and 6 are represented by solid lines while the imaginary components are represented by dashed lines. The values of ϵ_r' in Fig. 5 for the polyethylene, teflon, and lucite samples are seen to be in close agreement with the generally accepted values of 2.26, 2.10, and 2.60, respectively. As would be expected, $\mu_r' = 1$ was measured in all three cases.

Being low-loss dielectrics, one would expect to measure values of $\epsilon_r'' \sim 10^{-3}$ and $\mu_r'' \sim 0$ for these materials; however, Fig. 5 indicates that larger values were obtained for these parameters. The reason for this inconsistency is that for low-loss materials, i.e., $\epsilon_r'' < 0.05$ and $\mu_r'' < 0.05$, the mismatch at the stripline-to-coax joint and any impedance differences between the stripline and the network analyzer become the dominant factors in the *S*-parameter measurements and resulting calculations. The latter of these error sources also explains the slight periodic character of the ϵ_r' and μ_r' data. These conclusions were verified by making ϵ_r and μ_r measurements on the device while empty (air). It was found that tuning and detuning the coax to stripline matches lowered and raised, respectively, the measured values of ϵ_r'' and μ_r'' . The best matches obtained (Fig. 4) yielded values of ϵ_r'' and μ_r'' of ~ 0.03 . For this reason, the measurement technique was concluded to be inadequate for materials with ϵ_r'' and μ_r'' less than ~ 0.05 . By varying the width of the center conductor and, therefore, the impedance of the stripline, the amplitude of the periodic-like dependence of the measurements with frequency could be altered. By building the device as close to 50Ω as possible, the periodic character of the data can be minimized. For values of ϵ_r'' and μ_r'' greater than 0.05, these mismatch errors become insignificant. In general, the measurement technique was found to be accurate to better than ± 5 percent for all cases of ϵ_r and μ_r , excluding ϵ_r'' and μ_r'' less than 0.05.

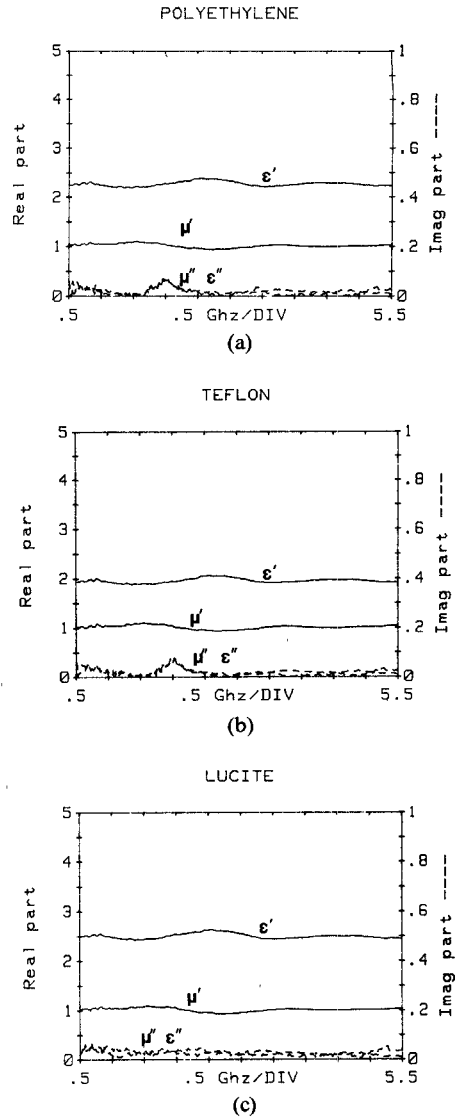


Fig. 5. ϵ_r and μ_r measured for several standard dielectrics.

It should also be pointed out that when first measured, the ϵ_r'' and μ_r'' data for these materials had sharp peaks at certain frequencies within the measurement band. In particular, there were resonant-like peaks at 2.5, 3.5, 4.3, and 5.0 GHz regardless of which material was being tested. The cause of these resonances was found to be the excitation of cavity modes inside the stripline chamber. The problem was solved by putting small blocks of RF absorber of the type found in anechoic chambers in each corner of the chamber (not shown in Fig. 2). The absorber blocks were positioned a large distance from the stripline center conductor where the TEM-wave fields can be considered to be negligible. Thus, the effect of the absorbers was to damp out the cavity modes while leaving the TEM mode unaltered. The effect of the absorbers was assessed by measuring ϵ_r and μ_r for the three dielectrics with and without the absorbers being present. In all three cases, the measured data was identical except for the spikes in ϵ_r'' and μ_r'' when the absorber was absent.

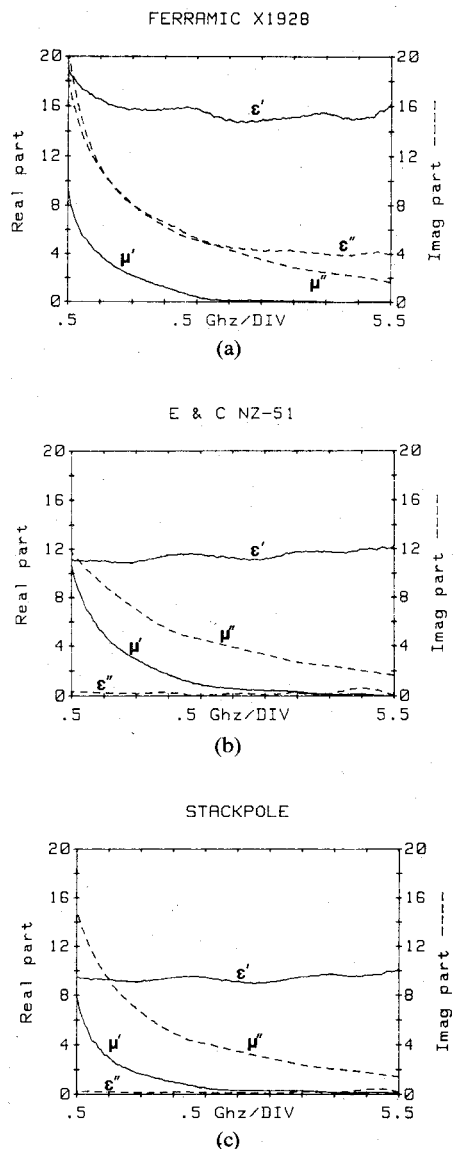


Fig. 6. ϵ_r and μ_r measured for several ceramic ferrites.

Permittivity and permeability for three different ferrite materials under consideration for the application described in [2] were measured with this technique. The measurement results appear in Fig. 6. The three ferrites—Ferramic 1928 (Indiana General), NZ-51 (Emerson and Cuming), and Stackpole (unknown type from Stackpole Corp.)—are all ceramic compositions used mainly in RF attenuation applications. As can be seen from Fig. 6, all three ferrites

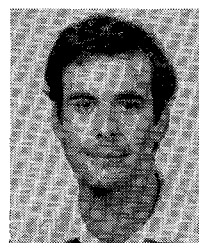
exhibit approximately the same properties with the exception of Ferramic 1928 which has a higher dielectric constant and loss tangent.

VI. SUMMARY

A broad-band automated technique for simultaneously measuring the real and imaginary components of ϵ_r and μ_r has been developed. The technique utilizes a strip transmission-line device loaded with the unknown material on which S-parameter measurements are made with an automated network analyzer. ϵ_r and μ_r are in turn computed from the measured S-parameters and have been found to be accurate to better than ± 5 percent. Some measured data for standard dielectrics and ceramic ferrites in the 0.5–5.5-GHz band have been presented. The measurement technique should be suitable for other materials with electromagnetic applications.

REFERENCES

- [1] W. B. Weir, "Automatic measurement of complex dielectric constant and permeability at microwave frequencies," *Proc. IEEE*, vol. 62, pp. 33–36, Jan. 1974.
- [2] W. C. Barry, "Suppression of propagating TE modes in the FNAL antiproton source stochastic beam cooling system," *IEEE Trans. Nucl. Sci.*, vol. NS-32, no. 5, Oct. 1985.
- [3] R. E. Collin, *Field Theory of Guided Waves*. New York: McGraw-Hill, 1960, ch. 3, pp. 79–83.
- [4] J. Smit and H. P. J. Wijn, *Ferrites*. New York: Wiley and Sons, 1959, ch. 7, pp. 132.



Walter Barry was born in Mamaroneck, NY, on May 16, 1959. He received the B.S. degree in physics and the M.S. degree in electrical engineering from the Georgia Institute of Technology in 1981 and 1982, respectively.

From 1979 to 1983, he was a research assistant at the Georgia Tech Engineering Experiment Station. From 1983 to 1984, he was an antenna engineer with the Harris Corporation in Melbourne, FL. Presently, he is a staff scientist with the University of California Lawrence Berkeley Laboratory, Berkeley, CA. He has worked in the areas of biomedical applications of microwaves, millimeter-wave devices and systems, and satellite communications. His current research interests are in electromagnetic devices for high-energy particle-beam monitoring and control.

Mr. Barry is a member of Sigma Pi Sigma, the Briarean Society, the American Institute of Physics, and the Optical Society of America.